ENSO related rainfall changes over the New Guinea region.

Ian Smith[1], Aurel Moise[1], Kasis Inape[2,] Brad Murphy[1], Rob Colman[1], Scott Power[1] and Christine Chung[1]

[1] CAWCR, Bureau of Meteorology

[2] Papua New Guinea National Meteorological Service

This article has been accepted for publication and undergone full peer review but has not been through the copyediting, typesetting, pagination and proofreading process which may lead to differences between this version and the Version of Record. Please cite this article as doi: 10.1002/jgrd.50818

Abstract

The large scale nature of El Niño-Southern Oscillation impacts on rainfall in the western Pacific region is generally well known but in some regions, where there are relatively few observations and the terrain is mountainous, the details of the impacts are less obvious. Here we analyze rainfall data for the New Guinea region comprising station observations, reanalysis products and satellite-based estimates in order to better understand some of these details. We find that most gridded products are limited due to their relatively coarse horizontal resolutions that fail to resolve topographic effects. However, the relatively fine resolution TRMM satellite–based product appears to provide reliable estimates and linear correlations between the data and the NINO34 sea surface temperature index provides an insight into the pattern of ENSO rainfall impacts. The first major finding is that the correlation patterns reveal that some highland regions are impacted differently to other surrounding regions, most likely because of the interaction between winds and topography. Secondly, we find that the association between ENSO and rainfall for stations in the New Ireland/New Britain region tends to be non-linear, in the sense that warm (El Niño)/cool (La Niña) events cause a decrease in rainfall – the strong 2010-2011 La Niña event being a clear example. Both findings help explain why previous studies have tended not to identify a simple large-scale response of New Guinea rainfall to ENSO.

1. Introduction

Figure 1 shows a map of New Guinea island which comprises both West Irian (WI) and Papua New Guinea (PNG). Papua New Guinea consists of the eastern half of the island and about 700 offshore islands between the equator and 12°S and 140°E and 160°E. Also shown

are the locations of two major off-shore islands - New Ireland and New Britain. The map illustrates the relatively high and complex topography that is a feature of the region as well as the locations of stations where relatively long-term, reliable rainfall records are available for analysis.

Based on an analysis of over 50 station records, McAlpine et al. (1983) estimated the pattern of annual mean rainfall and noted that the key features included dry (less than 2000 mm) zones along the southern and parts of the northern and eastern New guinea island coasts which contrasted with two inland wet (greater than 4000 mm) zones running west to east. McAlpine et al. (1983) noted that the wet regions tend to be those which have mountain ranges aligned transverse to the prevailing south easterly winds that predominate during May to August, and also that the New Britain region experiences a significant maximum rainfall on the northwest side of the island during summer, but an even larger rainfall maximum on the south eastern side during winter.

On the large scale, the average seasonal cycle of both rainfall and winds reflects the influence of the West Pacific Monsoon (WPM) (Smith et al., 2012) which can also be referred to as the Indonesian-Australian monsoon or the Indonesian Australian monsoon. It corresponds to the annual excursion of enhanced convection and low level westerly winds from India/Indo-China in July to Indonesia-Northern Australian in February (c.f. Lau and Chan, 1983; McBride et al., 2003; Chang et al., 2005).The seasonal cycle of rainfall for locations such as Port Moresby, for example, clearly reflects a wet season from November to April as a result of the WPM and a dry season from May to October when the region is exposed to dry south-easterly winds. Elsewhere, in locations such as Kavieng (New Ireland), the seasonal cycle of rainfall can be less distinct, depending on other factors including proximity to mountains,

coasts, and the positions and extents of the Intertropical Convergence Zone and the South Pacific Convergence Zone (Chang et al., 2005; Australian Bureau of Meteorology and CSIRO, 2011).

The general pattern of El Niño-Southern Oscillation (ENSO) impacts on rainfall patterns is reasonably well known at the large scale (e.g. McBride et al., 2003) but less so at the regional scale. This is also the case over much of the New Guinea region where station observations are relatively sparse, the topography is relatively complex and impacts appear to have a complex spatial structure. This was highlighted recently by the La Niña event of 2010-2011 when the general expectation was for above average rainfall over most of the region but actually was associated with severe drought in the New Ireland region, resulting in the deaths of five people as water supplies and crops dried up (The National (newspaper), Dry spell kills five in New Ireland, March 3, 2011).

Early studies into the nature of the impacts over Papua New Guinea include those by Nicholls (1973), McAlpine et al. (1983) and Allen et al. (1989a, b). Nicholls (1973) used available data from a relatively small number of stations and described the relationship between rainfall and the strength of the Walker circulation. He noted that a relatively weak circulation, such as in 1972, tends to favour above average rainfall in the central Pacific, in contrast with below average rainfall over the Indonesian Archipelago, and sometimes below average rainfall over much of West Irian and Papua New Guinea. He also noted that the relationship was far from uniform and that different regions could respond quite differently to El Niño and La Niña events in the central and eastern equatorial Pacific. While McAlpine et al. (1983) were able to describe the major features of mean PNG rainfall, they could not perform a reliable assessment of year-to-year rainfall variability because the available records were

too short. Allen et al. (1989 a, b) subsequently analyzed a longer data set and noted that that the links between PNG rainfall and ENSO indices were not particularly robust. More recently, the Australian Bureau of Meteorology and CSIRO (2011) describe the general nature of ENSO impacts on countries throughout the western tropical Pacific region and noted that Port Moresby tends to experience below average November to April rainfall during El Niño events. For PNG as a whole, only very strong eastern Pacific El Niño events show a clear impact (below average rainfall) and that for at least one station located in the north-east region (Kavieng), La Niña events lead to below average rainfall (B. Murphy, S. Power and S. McGree, The impacts of El Niño – Southern Oscillation and El Niño variations on Pacific island climates, submitted to Journal of Climate, 2013). Jourdain et al. (2013) found no significant correlation between all-New Guinea rainfall and the NINO34 index in various observational datasets and reanalyses during DJFM. They suggested that the effect of increased monsoon flow on moisture convergence during El Niño events could be counter-balanced by negative SST anomalies also induced by El Niño. Apart from these studies, very little has been published on the details of the impact of ENSO on the climate of PNG.

The aims of this paper are: (a) to assess how well gridded rainfall data products can capture the details of New Guinea rainfall patterns; (b) to better identify the nature and extent of ENSO events on New Guinea rainfall; and (c) to indicate the existence of a non-linear relationship between ENSO and rainfall in some regions. Section 2 describe these data, Section 3 provides a brief assessment of the rainfall climatologies, while Section 4 describes ENSO impacts evident in both station data and gridded data. Section 5 summarizes the main conclusions from this study.

2. Data

The Global Precipitation Climatology Centre (GPCC) provides a high resolution (0.5 deg.) product for the global land surface based on an interpolation of gauge measurements (Schneider et al., 2011). This comprehensive data base makes use of measurements going back as far as 1901. For the period 1980 to 2010, well over 60 stations contributed to the analyses over New Guinea but most of these contributed less than 100% of the time. Many of these stations have closed down and far fewer reliable, long-term station records are available for analysis nowadays. For example, for the month of December 2010, 14 stations in West Irian, and only 7 PNG stations contributed to the GPCC analysis (not shown).

In addition to the GPCC land station-only data, a variety of gridded rainfall products (see Table 1) are now available. Reanalysis products (e.g. NCEP1) provide rainfall estimates at varying spatial resolutions but the quality of these values can be affected by the limitations associated with the methods used to parameterize convective rainfall and assimilate the observations of atmospheric variables (e.g. temperature, humidity, pressure, surface winds etc.). Satellite-based rainfall estimates can assist rainfall and hydrological studies where sparse observations are a problem. The CPC Merged Analysis of Precipitation (CMAP) data (Xie, and Arkin, 1997) and the Global Precipitation Climatology Project (GPCP) data (Adler et al., 2003) both comprise satellite based estimates over the oceans and the interpolation of available rain gauge measurements over land. However, as in the case of the GPCC product, the quality of the gridded rainfall data is limited by the number and quality of station observations.

These data are complemented by the Tropical Rainfall Measurement Mission (TRMM) monthly dataset (3B43) which provides satellite-only based rainfall estimates for the entire tropical belt (50°S to 50°N) at a much greater horizontal resolution of 25 km (Huffman et al., 2009). The TRMM data have been assessed and used over several regions including Africa (Adeyewa and Nakamura, 2003; Nicholson et al. 2003a,b, Hughes, 2006), the Amazon Basin (Buarque et al., 2011; Clarke et al., 2011, Collischonn et al., 2008, Getirana et al., 2011), Australia (Ebert et al., 2007; Fleming et al., 2011), Cyprus (Gabella et al., 2006), Oklahoma (Fisher, 2004), Iran (Javanmard et al., 2010) and Peru (Condom et al., 2011). For example, Zhou and Wang (2006) used TRMM data to study the diurnal cycle of rainfall over the New Guinea region and identified the relatively complex interaction between convective activity, land-sea breezes and orography. Chang et al. (2005) used TRMM data to demonstrate a strong relationship between rainfall and winds over much of south-east Asia, including West Irian.

The horizontal resolution of these products varies by an order of magnitude, which means that the products differ in their ability to resolve rainfall features. The CMAP and GPCP products are available at a resolution of 250 km and extend over 29 years. The TRMM data is of much higher spatial resolution (25km) but it is only available for a shorter period (1999 to 2011).

We have also collected monthly rainfall records from a number of stations throughout both Papua New Guinea (15) and West Irian (4) (Table 2). These are long-term records, but are not always continuous nor complete. Nevertheless, we have assembled seasonal (i.e. JFM, AMJ, JAS and OND) rainfall totals for as many years as possible post-1950. Where there are

isolated missing values, we have infilled using the estimates of the long-term average monthly mean values

Finally, in this study we use the NINO34 sea surface temperature (SST) index as measure of the strength of ENSO events. This index is defined as the average of SST anomalies over the region 5°N –to 5°S and 170° W to 120°W. Monthly NINO34 values were obtained from NOAA (NOAA, 2013).

3. Wet and dry season rainfall

Figure 2 shows estimates of the wet season (October to April) mean rainfall from each of the observed and reanalysis gridded rainfall products. The CMAP estimates indicate a relatively simple pattern, with very few values less than about 5 mm per day or greater than about 10 mm per day over the central mainland. The GPCP estimates resemble the CMAP pattern of values over land, but tend to be drier over the surrounding ocean points. This might be explained by the different methods used to retrieve the raw satellite data. The NCEP1 estimates are also similar to CMAP and GPCP values over much of the land, but are drier over the surrounding ocean points. NCEP2 estimates also resemble the CMAP values but, in this case, tend to be wetter, especially over the highland regions. The ERA40 estimates appear unrealistic since maximum values exceed 20 mm per day over two large inland regions and are not supported by any station observations. ERA-INT estimates, on the other hand, appear more realistic since the patterns appear to reflect the effects of the underlying topography. The MERRA estimates also better reflect the existence of the central highlands but the values appear excessive, exceeding 20 mm per day over much of the mainland. The CFSR estimates, at a resolution of only 50km, appear strongly affected by the topography but

also appear problematic since the pattern is dominated by alternating regions of maxima and minima which are not evident in any station observations or other estimates. The GPCC features include evidence for two bands of maxima lying across the mainland and a maximum just to the west of New Britain. The TRMM estimate also clearly indicates two bands of rainfall maxima and a maximum over western New Britain. In general, the ERA-INT re-analysis product, the station-based GPCC product and the TRMM satellite-based product appear consistent when allowing for differences in horizontal resolution and the fact that direct station observations are relatively sparse.

Figure 3 compares the estimates for the dry season (May to September) rainfall. The CMAP product again indicates a relatively simple pattern, with minima less than 1 mm per day in the very far south contrasting with maxima greater than 12 mm per day in the far north east. The GPCP estimates are similar, except that they indicate a maximum to the east of New Britain and are not as wet in the north east. The NCEP1 and NCEP2 estimates do not reflect this feature, but instead indicate a more centrally located maximum over the mainland. The ERA40 does indicate a maximum to the east of New Britain but, as with the wet season, appears to severely overestimate rainfall across much of the mainland. The ERA-INT product appears more consistent with the CMAP and GPCP rainfall estimates and includes features that appear to represent topographic effects. The MERRA product again also indicates a strong topographic effect but, as with wet season rainfall and like ERA40, appears too wet. The CFSR product again appears unrealistic, possibly due to a problem with spectral representation of topography. The GPCC product provides confirmation of the maximum to the east of New Britain, and the existence of maxima over the mainland which is also seen in the TRMM data. Again, if we allow for differences in horizontal resolution, and the sparseness of station observations, it appears that the ERA-INT, GPCC and TRMM products

are consistent. However, it is worth noting that the TRMM values may be too low over the oceans to the north. It is also worth noting that, while increasing resolution tends to improve the representation of topography, it does not necessarily improve the representation of rainfall. The MERRA and CFSR products appear less realistic than the coarser resolution ERA-INT product.

One of the main differences between the wet and dry seasons is the shift in the position of the rainfall maximum from west to east of New Britain. As noted by McAlpine et al. (1983), this occurs because of the reversal of winds from north westerlies during the summer season to south easterlies during the winter season. This is evident in each of the ERA-INT, GPCC and TRMM products. A second major difference revealed by the high resolution TRMM data, and which is not clear in the other two data sets, is the disappearance of one of the two rainfall maxima bands that lie across the mainland during the wet season. This feature, which is evident in the McAlpine et al. (1983) analysis, most likely reflects the interaction between the prevailing winds, the topography and the existence of rain shadow effects.

4. ENSO impacts

ENSO events tend to develop and mature between austral winter (JJA) and spring (SON), peak during summer (DJF) and decay by autumn (MAM). Rainfall over the Maritime Continent tends to be below average in El Niño years (Ramage, 1968) but it has been noted that the relationship between PNG rainfall and ENSO indices is not robust and that only very strong El Niño events appear to have a clear impact (Allen et al. 1989 a, b; Jourdain et al. 2013). These findings can occur if (a) there is no strong relationship to begin with; (b) ENSO impacts vary considerably at the smaller scales and any attempt at large scale averaging

effectively makes them disappear; or (c) the relationship is non-linear. With respect to the latter, this can readily occur as a consequence of the movement of a local rainfall maximum away from its normal position (e.g. Hoerling et al. 1997, 2001; Power et al. 2006; C. T.Y. Chung, S.B. Power, J.M. Arblaster, H.A. Rashid, and G.L. Roff, Nonlinear rainfall response to El Niño and global warming in the Indo-Pacific, submitted to *Climate Dynamics*, 2013). In this situation, it does not matter whether the movement is to the east (during El Niño events) or to the west (during La Niña events), the underlying regions will always tend to experience decreases and any linear relationship with ENSO events is likely to be non-existent.

In order to test these explanations, we have used selected gridded rainfall products to calculate the linear correlation between seasonal rainfall and the NINO34 index. The two products we use are the CMAP and TRMM data sets (Table 1). The CMAP data is coarse resolution (250 km), relies on available station observations over land, but has the advantage of extending back to 1980. The TRMM data is based solely on satellite data, is high resolution (25km), but only extends back to 1998. Furthermore, because of the different sample sizes associated with the two data sets, we only display those correlation values that are estimated to be statistically significant at the $p<.10$, $p<.05$ and $p<0.01$ levels.

Figure 4 shows the results from CMAP data for each of the 3-month seasons January to March (JFM), April to June (AMJ), July to September (JAS) and October to December (OND). The main feature is the evidence for a predominantly negative association (i.e. reduced rainfall with warmer NINO34 sea surface temperatures) over most of the region for all seasons except for the New Ireland and New Britain regions where the association tends to be positive during JFM and AMJ. The strongest and most widespread negative associations occur during early summer (OND) when most correlations are significant ($p<.05$). During the

remainder of the year there is almost no evidence for correlations over land points that are better than $p<0.10$. These results are not particularly unique, since they broadly reflect the large scale patterns identified in other studies such as McBride et al. (2003, Figure 2) who analysed gridded outgoing long-wave radiation (OLR) data (1974 to 2001), or Chang et al. (2005, Figure 2) who correlated CMAP DJF rainfall with NINO3 SST anomalies.

The results from the TRMM data (Figure 5) are roughly similar to the CMAP results in that they indicate a large scale pattern of negative associations in the south and west contrasting with positive associations to the north east. Again, the strongest and most widespread negative associations occur during OND. However, the results differ substantially in a number of respects. For example, the southern highland regions (including Port Moresby) tend to experience significant negative associations in all seasons except AMJ, while the northern highlands tend to experience positive associations during JFM and JAS. The sharp contrast seen during JFM highlights the effect of topography which is non-existent in the CMAP results. The New Britain region also exhibit contrasts contrast during JAS and OND when negative associations occur in the south and west and positive associations occur to the north and east. Again, these detailed features of the associations are either very weak or non-existent in the CMAP results. This is to be expected since the CMAP data involves data from sparse station observations over land which have been interpolated and averaged up to a coarse scale resolution of 250 km.

Are the TRMM-based associations consistent with the results from individual station data? Table 2 shows the ENSO associations calculated for a number of stations where reliable long-term data was available for analysis. It shows, for each station, the number of years where seasonal averages were calculated and the corresponding correlation coefficients. The

number of years varies from as few as 15 (Vanimo) to as many as 62 (Misima) and the level of statistical significance associated with each correlation varies accordingly. The results are summarized in Figure 6 which indicates where and when the associations are significantly ($p<.05$) negative or positive. Taking into account the years involved in calculating the correlations are both different and often non-overlapping, the station-based estimates are consistent with the TRMM-based estimates insofar as they reflect the general south-west to north-east contrast in associations, with the positive associations tending to cluster around New Britain and the north-eastern slopes on the mainland.

In the case of four stations (Momote, Kavieng, Rabaul/Tokua and Hoskins) in the New Ireland and New Britain regions, Table 2 also includes the correlation coefficients associated with second-order polynomial fits between the seasonal rainfall and NINO34 values. These coefficients are always positive and the level of statistical significance reflects the fact that the number of degrees of freedom is less than that for a linear fit. Figure 6 identifies where these non-linear fits to the data are much more significant than the linear fits while Figures 7 to 10 indicate why this is the case by showing the individual scatter plots of the data. In the case of Momote (Figure 7) there are no significant linear associations but there is a significant non-linear association during JFM which can be seen to arise because of a tendency for the rainfall totals to decrease when the NINO34 SST is either relatively warm or relatively cool. The situation at Kavieng (Figure 8) is even more pronounced, where non-linear associations are significant in all four seasons, and highly significant (i.e. $p<.01$) during JFM and AMJ. Again, the association corresponds to a decrease in rainfall when the NINO34 SST is either relatively warm or relatively cool. The same effect is seen at Rabaul/Tokua (Figure 9) where the non-linear associations explain much more of the interannual variance in rainfall than do the linear associations. At Hoskins (Figure 9) where the sample comprises

only 16 years, the picture is less clear. There is no great difference between linear or non-linear associations except, perhaps, during OND. These non-linear associations are robust since they are evident in the data from all four stations in almost all of the four seasons.

One of the strongest La Niñas on record occurred in 2010/2011 and, in accordance with the associations evident in Figure 5, rainfall was below average for the New Ireland/New Britain regions. Based on station data, Figures 7 to 10 show that it actually led to quite severe rainfall deficiencies. Momote recorded well below average rainfall in both OND, 2010 and JFM, 2011 (Figure 7) and, while the same was seen at Kavieng (Figure 8) it continued to suffer for another 3 months into AMJ, 2011. The situation at Rabaul/Tokua (Figure 9) appears even worse, since it experienced below average rainfall for an entire 12 months JAS, 2010 through until AMJ, 2011. Hoskins fared better, experiencing below average rainfall for only 6 months JFM, 2011 to AMJ, 2011 (Figure 10).

5. **Discussion and conclusions**

The climate of the New Guinea region is relatively complex as a result of the interactions between important factors such as topography, the Western Pacific monsoon and ENSO. This results in detailed rainfall patterns which are not well resolved by the relatively sparse and sometimes incomplete station observations. Available rainfall products, such as those based on observations or reanalysis data can be limited by relatively coarse horizontal resolution but the high resolution TRMM rainfall estimates appear reliable since they are consistent with both available station observations and reanalysis estimates.

In terms of understanding the nature of the rainfall –NINO34 SST associations seen in the TRMM data (Figure 6), it is important to recognize that rainfall at any location is dependent on several factors which are not investigated in detail here but most likely reflect the interaction between changes to the local wind regimes and topography. This is evident in the patterns over the mainland where the associations can change sign from the southern slopes to the northern slopes while, in the vicinity of New Britain and New Ireland, the data also indicate that the associations can change sign in going from west to east.

McBride et al (2003, Figure 2) showed correlation maps between outgoing long-wave radiation and the Southern Oscillation at the monthly time scale which provide an indication of the rainfall-ENSO relationship at the large scale. These tend to indicate a relatively simple pattern of positive correlations to the north and east which contrast with negative correlations to the west and south. According to the maps for January, October, and possibly July, it would seem reasonable to expect that average mainland rainfall should be significantly correlated with ENSO. The fact that previous studies based on large scale averages have not detected any such correlations implies a more complex picture at smaller scales. This is confirmed by the TRMM-based results which highlight the existence of both contrasting correlations and relatively weaker correlations over the highland regions compared to elsewhere. This is most evident in January to March (Figure 5a) which reveals a zero isoline that effectively runs from the south-east through to the far west of the mainland and beyond, and appears associated with significant positive correlations over some highland regions. This is very different to the McBride et al. (2003) pattern during January, which involves a zero isoline that effectively runs north-south to the east of the mainland. That this occurs is not particularly surprising given the close relationship between wind direction and rainfall in the vicinity of mountains and the fact that ENSO events do not just involve movements in the

centers of convection, but also involve changes to wind strength and direction. As a consequence, these findings indicate that the failure to identify a simple robust signal in previous studies is most likely due to the fact that the impacts vary considerably over relatively small spatial scales but effectively disappear when attempting to create a regional scale average (Chang et al., 2005).

In addition, station data from the New Ireland/New Britain region indicates the existence of a strong non-linear association between rainfall and NINO34 SSTs. The dry conditions experienced in the New Ireland/New Britain region during 2010/2011 can be readily understood in terms of the regional rainfall maximum shifting west in response to La Niña conditions. Similarly, the data imply that dry conditions can also occur in response to the maximum shifting east in response to El Niño conditions, an effect seen in other regions countries including Australia (Power et al., 2006), New Zealand (Mullan, 1996) and several other Pacific island nations (B. Murphy, S. Power and S. McGree, The impacts of El Niño – Southern Oscillation and El Niño variations on Pacific island climates, submitted to Journal of Climate, 2013). This feature will also have contributed to the failure of previous studies to identify a simple robust ENSO-related signal based on simple linear regression.

Finally, the limitations of relatively coarse horizontal resolution products, as evidenced by the results presented here, again highlights the danger of using large-scale results from climate models to infer values at smaller, unresolved scales. In particular, there is a tendency to use the results from climate model simulations to infer changes in climate (due to enhanced greenhouse gas concentrations) at point locations when, in many cases, the models do not adequately resolve important topographic features (Smith, 2013) The same potential problem may apply to seasonal climate predictions where it is likely that extrapolating the impacts of

ENSO from one region to another will be misleading in the absence of direct observations (Chang et al.;2005).

Acknowledgements

This research was supported by the Pacific Climate Change Science and Adaption Program (PCCSAP), a program supported by AusAID, in collaboration with the Department of Climate Change and Energy Efficiency, and delivered by the Bureau of Meteorology and the Commonwealth Scientific and Industrial Research Organisation (CSIRO). The authors would like to thank Dewi Kirono for kindly providing access to the rainfall observations for stations in West Irian,and Hahn Ngyuen and Nicolas Jourdain for providing very useful comments on an early draft of this paper. Two anonymous reviewers also provided valuable feedback on a version of the manuscript.

References

Adeyewa, Z. D., & Nakamura, K. (2003). Validation of TRMM radar rainfall data over major climatic regions in Africa. *Journal of Applied Meteorology*, 42(2), 331-347.

Adler, R.F., G.J. Huffman, A. Chang, R. Ferraro, P. Xie, J. Janowiak, B. Rudolf, U. Schneider, S. Curtis, D. Bolvin, A. Gruber, J. Susskind, P. Arkin and E. Nelkin (2003) The Version 2 Global Precipitation Climatology Project (GPCP) Monthly Precipitation Analysis (1979-Present). *J. Hydrometeor.*, 4, 1147-1167.

Allen, B. H. Brookfield and Y.Byron, (1989a) Frost and Drought through Time and Space, Part I: The Climatological Record. *Mountain Research and Development*, 9(3), 252-278.

Allen, B. H. Brookfield and Y. Byron, (1989b) Frost and Drought through Time and Space, Part II: The Written, Oral, and Proxy Records and Their Meaning. *Mountain Research and Development*, 9(3), 279-305.

Australian Bureau of Meteorology and CSIRO (2011) Climate Change in the Pacific: Scientific assessment and new research. Volume 1: Regional Overview, 257 pp.

Buarque, D. C., de Paiva, R. C. D., Clarke, R. T., & Mendes, C. A. B. (2011). A comparison of Amazon rainfall characteristics derived from TRMM, CMORPH and the Brazilian national rain gauge network. Journal of Geophysical Research: Atmospheres (1984–2012), 116(D19).

Chang, C. P., Wang, Z., McBride, J., & Liu, C. H. (2005). Annual cycle of Southeast Asia-Maritime Continent rainfall and the asymmetric monsoon transition. Journal of climate, 18(2), 287-301.

Clarke, R. T., Buarque, D. C., de Paiva, R. C. D., & Collischonn, W. (2011). Issues of spatial correlation arising from the use of TRMM rainfall estimates in the Brazilian Amazon. Water Resources Research, 47(5).

Collischonn, B., Collischonn, W., & Tucci, C. E. M. (2008). Daily hydrological modeling in the Amazon basin using TRMM rainfall estimates. Journal of Hydrology, 360(1), 207-216.

Condom, T., Rau, P., & Espinoza, J. C. (2011). Correction of TRMM 3B43 monthly precipitation data over the mountainous areas of Peru during the period 1998–2007. Hydrological Processes, 25(12), 1924-1933.

Dee, D. P., Uppala, S. M., Simmons, A. J., Berrisford, P., Poli, P., Kobayashi, S., ... & Vitart, F. (2011). The ERA-Interim reanalysis: Configuration and performance of the data assimilation system. Quarterly Journal of the Royal Meteorological Society, 137(656), 553-597.

Ebert, E. E., Janowiak, J. E., & Kidd, C. (2007). Comparison of near-real-time precipitation estimates from satellite observations and numerical models. Bulletin of the American Meteorological Society, 88(1), 47-64.

Fisher, B. L. (2004). Climatological validation of TRMM TMI and PR monthly rain products over Oklahoma. Journal of applied meteorology, 43(3), 519-535.

Fleming, K., Awange, J. L., Kuhn, M., & Featherstone, W. E. (2011). Evaluating the TRMM 3B43 monthly precipitation product using gridded raingauge data over Australia. Australian Meteorological and Oceanographic Journal, 61(3), 171.

Gabella, M., Michaelides, S. C., Constantinides, P., & Perona, G. (2006). Climatological validation of TRMM precipitation radar monthly rain products over Cyprus during the first 5 years (December 1997 to November 2002). Meteorologische Zeitschrift, 15(5), 559-564.

Getirana, A. C. V., Espinoza, J. C. V., Ronchail, J., & Rotunno Filho, O. C. (2011). Assessment of different precipitation datasets and their impacts on the water balance of the Negro River basin. Journal of Hydrology, 404(3), 304-322.

Haylock, M., & McBride, J. (2001). Spatial coherence and predictability of Indonesian wet season rainfall. Journal of Climate, 14(18), 3882-3887.

Hoerling, M. P., Kumar, A., & Zhong, M. (1997). El Niño, La Niña, and the nonlinearity of their teleconnections. Journal of Climate, 10(8), 1769-1786.

Hoerling, M. P., Kumar, A., & Xu, T. (2001). Robustness of the nonlinear climate response to ENSO's extreme phases. Journal of Climate, 14(6), 1277-1293.

Huffman, G. J., Adler, R. F., Bolvin, D. T., & Gu, G. (2009). Improving the global precipitation record: GPCP version 2.1. Geophysical Research Letters, 36(17).

Hughes, D. A. (2006). Comparison of satellite rainfall data with observations from gauging station networks. Journal of Hydrology, 327(3), 399-410.

Javanmard, S., Yatagai, A., Nodzu, M. I., BodaghJamali, J., & Kawamoto, H. (2010). Comparing high-resolution gridded precipitation data with satellite rainfall estimates of TRMM_3B42 over Iran. Advances in Geosciences, 25(25), 119-125.

Jourdain, N. C., Gupta, A. S., Taschetto, A. S., Ummenhofer, C. C., Moise, A. F., & Ashok, K. (2013). The Indo-Australian monsoon and its relationship to ENSO and IOD in reanalysis data and the CMIP3/CMIP5 simulations. Climate Dynamics, 1-30.

Kalnay, E., Kanamitsu, M., Kistler, R., Collins, W., Deaven, D., Gandin, L., ... & Joseph, D. (1996). The NCEP/NCAR 40-year reanalysis project. Bulletin of the American meteorological Society, 77(3), 437-471.

Kanamitsu, M., Ebisuzaki, W., Woollen, J., Yang, S. K., Hnilo, J. J., Fiorino, M., & Potter, G. L. (2002). Ncep-doe amip-ii reanalysis (r-2). Bulletin of the American Meteorological Society, 83(11), 1631-1643.

Kirono, D. G., Tapper, N. J., & McBride, J. L. (1999). Documenting Indonesian rainfall in the 1997/1998 El Niño event. Physical Geography, 20(5), 422-435.

Lau, K. M., & Chan, P. H. (1983). Short-term climate variability and atmospheric teleconnections from satellite-observed outgoing longwave radiation. Part I: Simultaneous relationships. Journal of the atmospheric sciences, 40(12), 2735-2750.

McAlpine, J.R., G. Keig and R. Falls, (1983) Climate of Papua New Guinea. CSIRO, Australian National University Press, 200p.

McBride, J. L., Haylock, M. R., & Nicholls, N. (2003). Relationships between the Maritime Continent heat source and the El Niño-Southern Oscillation phenomenon. Journal of climate, 16(17), 2905-2914.

Mullan A.B. (1996) Non-linear effects of the southern oscillation in the New Zealand region. *Aus. Met. Mag*., 45, 83–99

Nicholls, N. (1973) The Walker Circulation and Papua New Guinea rainfall. Bureau of Meteorology Technical Report 6, September 1973.

Nicholson, S. E., Some, B., McCollum, J., Nelkin, E., Klotter, D., Berte, Y., ... & Traore, A. K. (2003a). Validation of TRMM and other rainfall estimates with a high-density gauge dataset for West Africa. Part I: Validation of GPCC rainfall product and pre-TRMM satellite and blended products. Journal of Applied Meteorology, 42(10), 1337-1354.

Nicholson, S. E., Some, B., McCollum, J., Nelkin, E., Klotter, D., Berte, Y., ... & Traore, A. K. (2003). Validation of TRMM and other rainfall estimates with a high-density gauge dataset for West Africa. Part II: Validation of TRMM rainfall products. Journal of Applied Meteorology, 42(10), 1355-1368.

NOAA, (2013) Table of climate indices at http://www.cpc.ncep.noaa.gov/data/indices/ersst3b.nino.mth.81-10.ascii, accessed on July 31, 2013.

Power, S., Haylock, M., Colman, R., & Wang, X. (2006). The predictability of interdecadal changes in ENSO activity and ENSO teleconnections. Journal of Climate, 19(19), 4755-4771.

Ramage, C.S. (1968) The role of the "Maritime Continent" in the atmospheric circulation. Monthly Weather Review, 96, 365-369.

Saha, S., Moorthi, S., Pan, H. L., Wu, X., Wang, J., Nadiga, S., ... & Reynolds, R. W. (2010). The NCEP climate forecast system reanalysis. Bulletin of the American Meteorological Society, 91(8), 1015-1057.

Schneider, U., A. Becker, P. Finger, A. Meyer-Christoffer, B. Rudolf, and M. Ziese, (2011) GPCC Full Data Reanalysis Version 6.0 at 0.5°: Monthly Land-Surface Precipitation from Rain-Gauges built on GTS-based and Historic Data. DOI: 10.5676/DWD_GPCC/FD_M_V6_050

Smith, I. N., Moise, A. F., & Colman, R. A. (2012). Large-scale circulation features in the tropical western Pacific and their representation in climate models. Journal of Geophysical Research, 117(D4), D04109.

Smith, I., Moise, A., Katzfey, J., Nguyen, K., & Colman, R. (2013). Regional scale rainfall projections: Simulations for the New Guinea region using the CCAM model. Journal of Geophysical Research: Atmospheres.

Xie, P., & Arkin, P. A. (1997). Global precipitation: A 17-year monthly analysis based on gauge observations, satellite estimates, and numerical model outputs. Bulletin of the American Meteorological Society, 78(11), 2539-2558.

Zhou, L., & Wang, Y. (2006). Tropical Rainfall Measuring Mission observation and regional model study of precipitation diurnal cycle in the New Guinean region. Journal of Geophysical Research: Atmospheres (1984–2012), 111(D17).

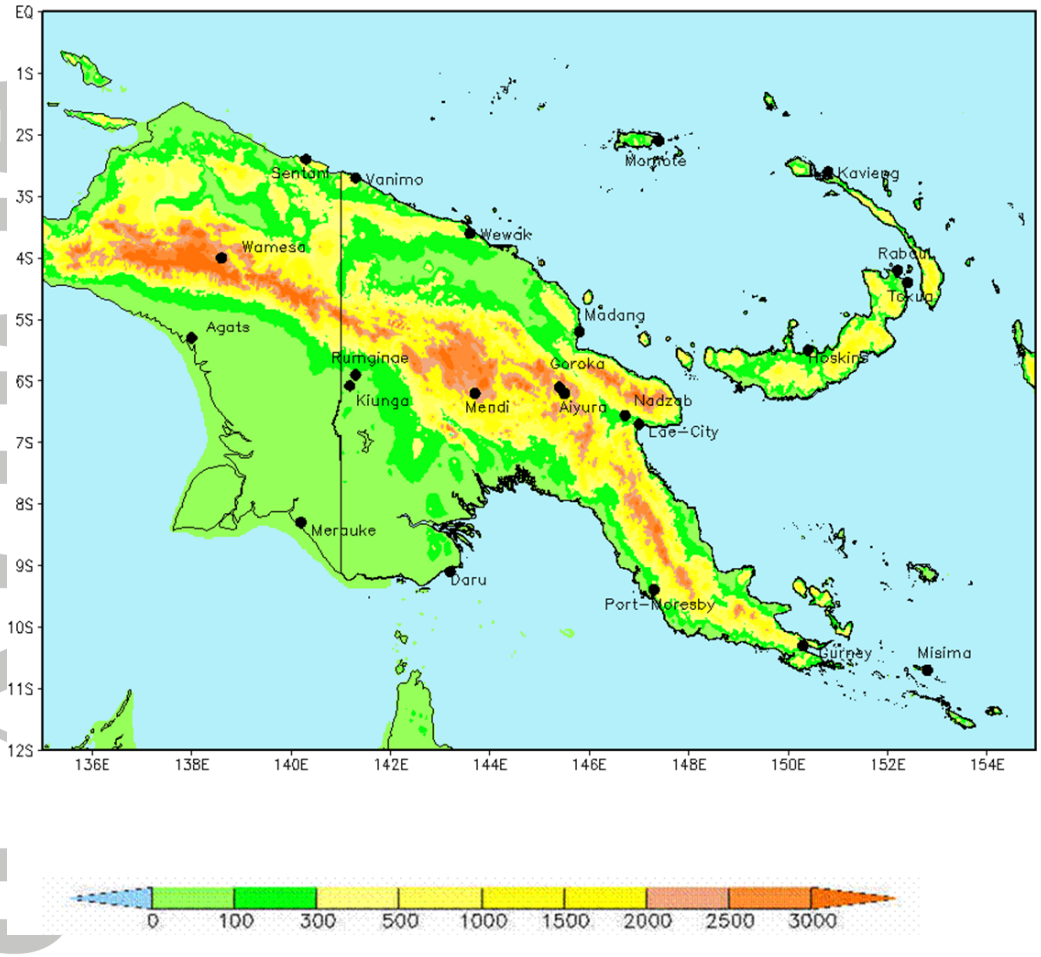

Figure 1. The wider New Guinea region indicating topography (meters above sea level) and locations of 20 stations where reliable, ongoing rainfall records have been used in this study. Source: ETOPO2v2 global gridded 2-minute database (National Geophysical Data Center, National Oceanic and Atmospheric Administration, U.S. Dept. of Commerce, http://www.ngdc.noaa.gov/mgg/global/etopo2.html)

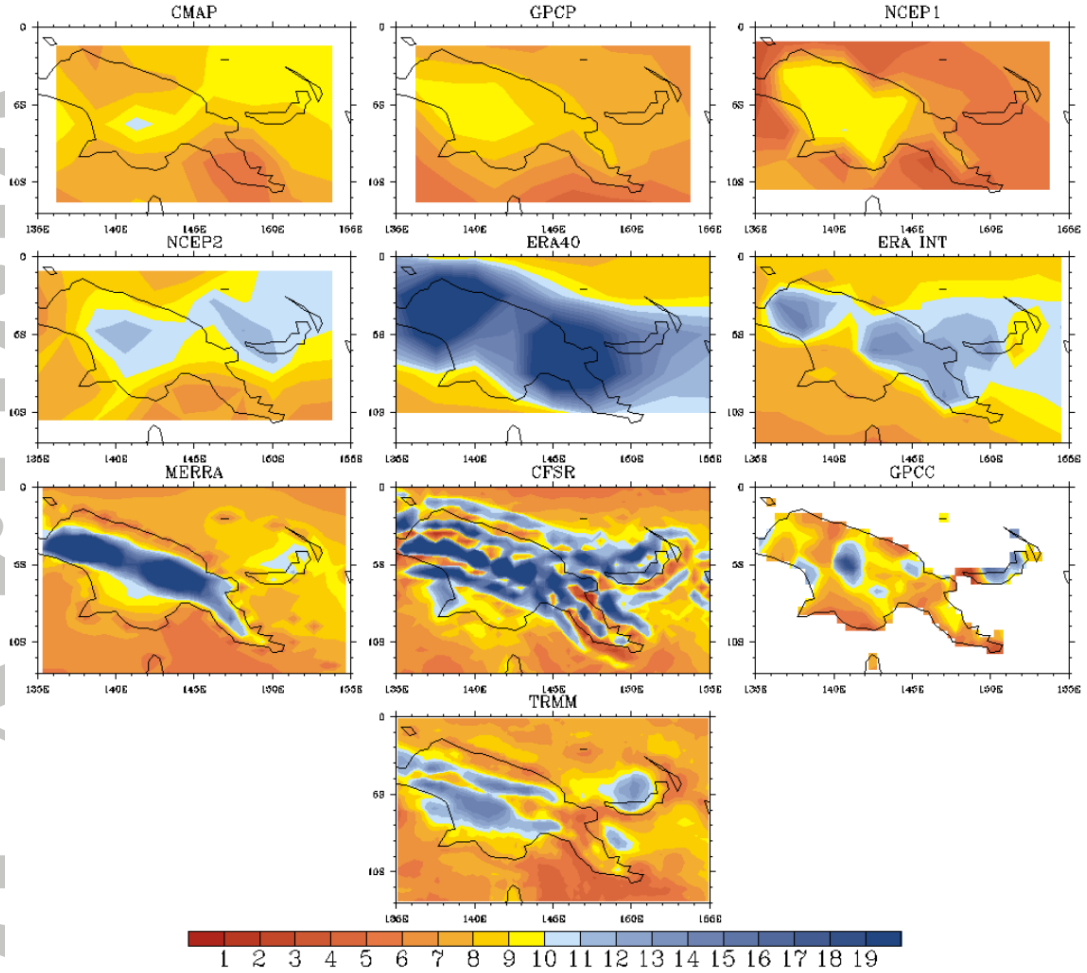

Figure 2. Estimates of October to April mean rainfall (mm per day) from each of the nine observational and reanalysis datasets.

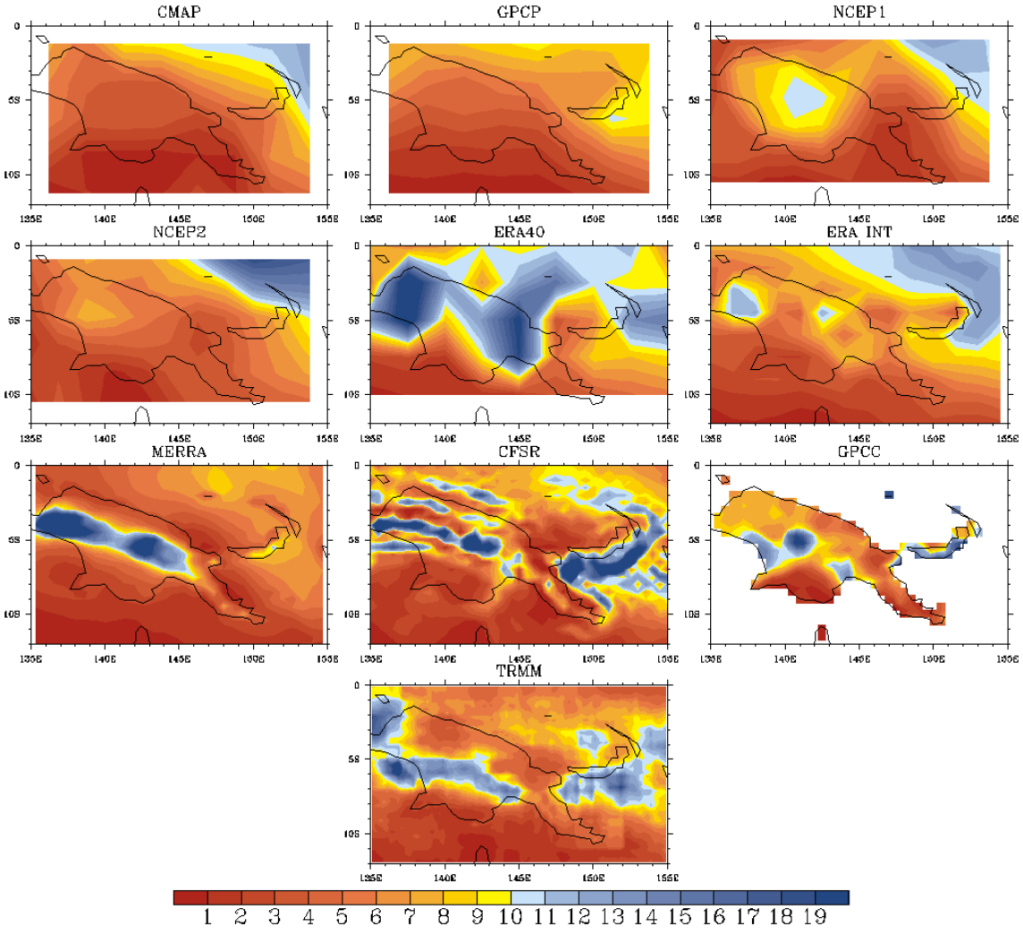

Figure 3. As for Figure 3 except for May to September.

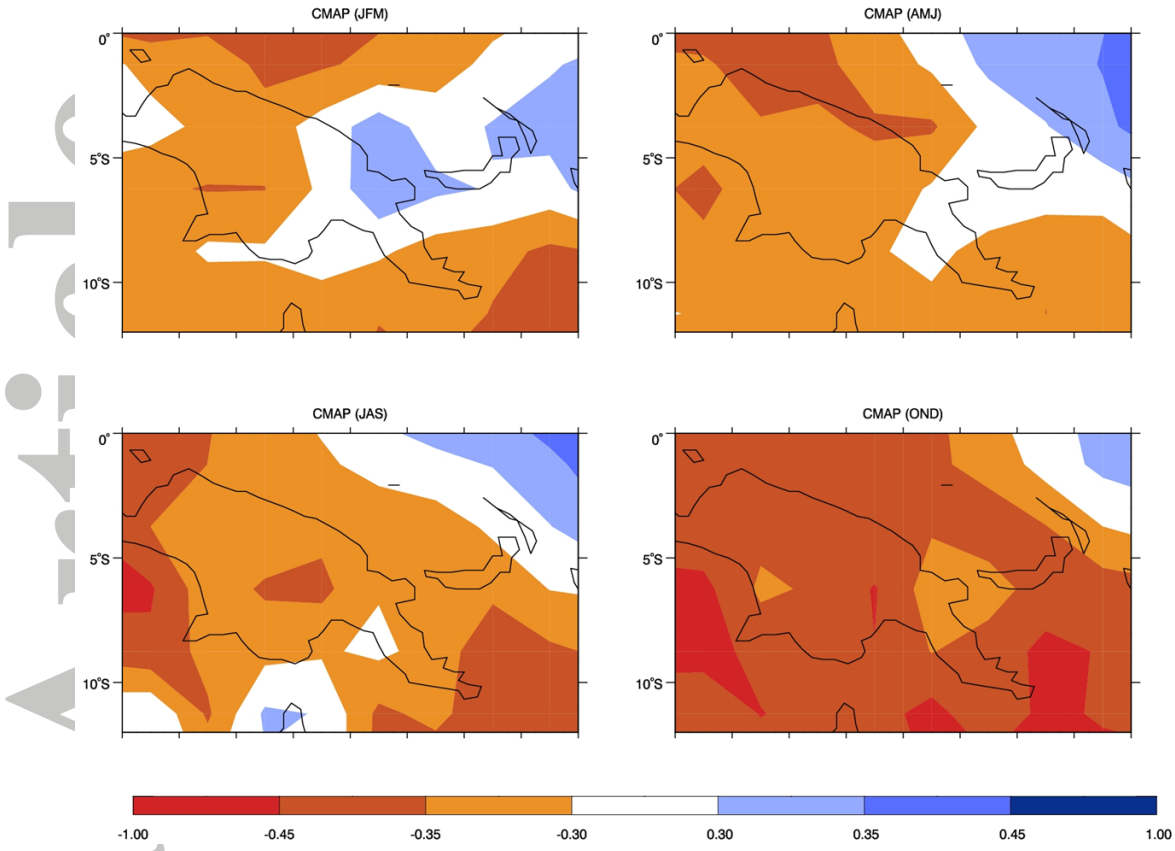

Figure 4. Correlations between CMAP seasonal rainfall and NINO34 SST anomalies (1980 to 2008)

(a) JFM (b) AMJ (c) JAS and (d) OND.

Values greater than 0.30, 0.35 and 0.45 in magnitude correspond to significance levels $p<0.1$, <0.05 and <0.01 respectively.

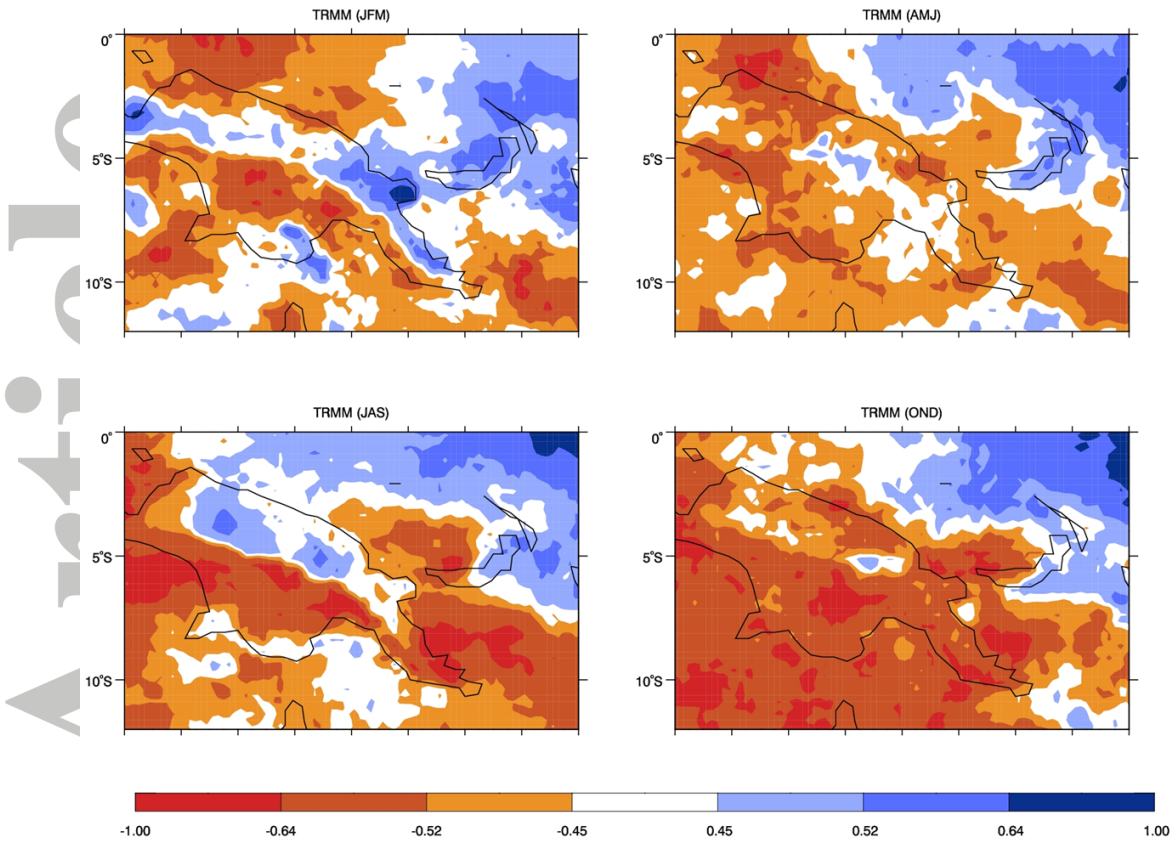

Figure 5. As for Figure 4 except for TRMM seasonal rainfall (1998 to 2011).

Values greater than 0.45, 0.52 and 0.64 in magnitude correspond to significance levels $p<0.1$, <0.05 and <0.01 respectively.

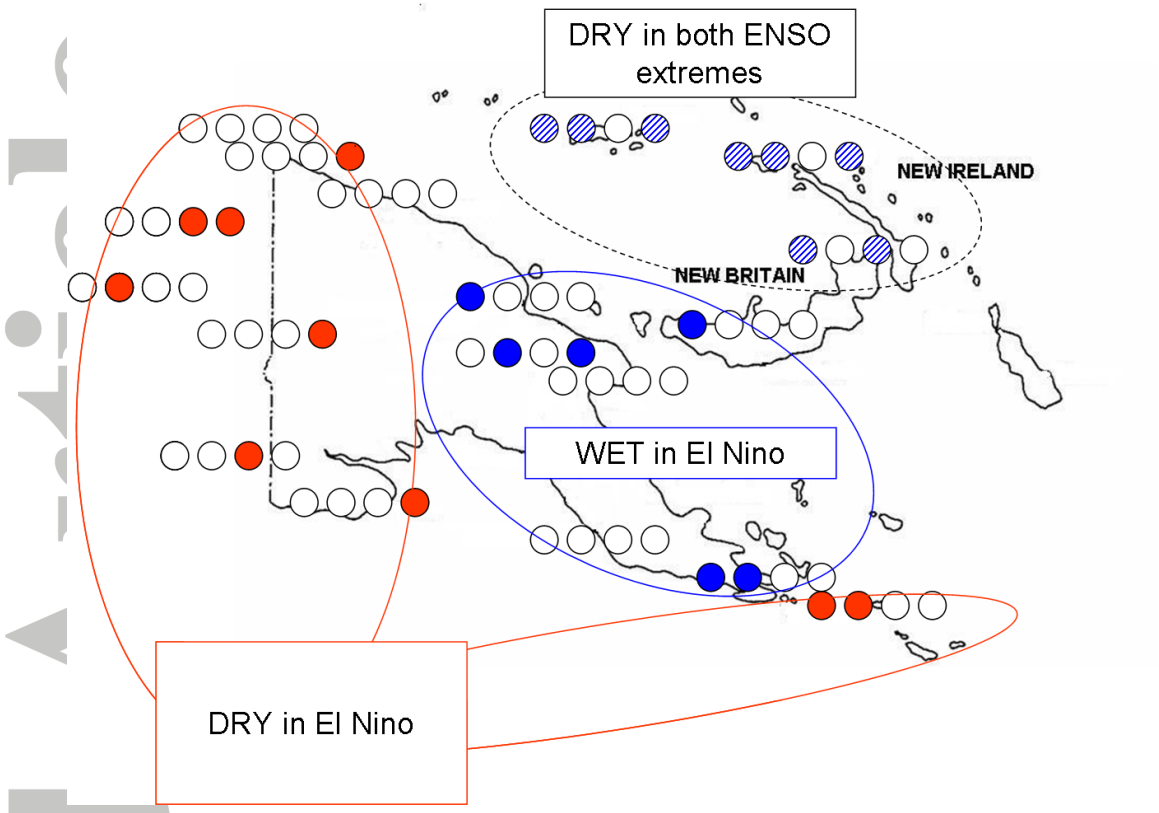

Figure 6. Relationships between station seasonal rainfall totals and the NINO34 SST anomalies (see Table 2). The four circles correspond to JFM, AMJ, JAS and OND seasons respectively. Red indicates a significant (i.e. $p<.05$) negative association, blue a significant positive association, and white no significant association. A blue hatched circle denotes a significant second order polynomial fit to the data.

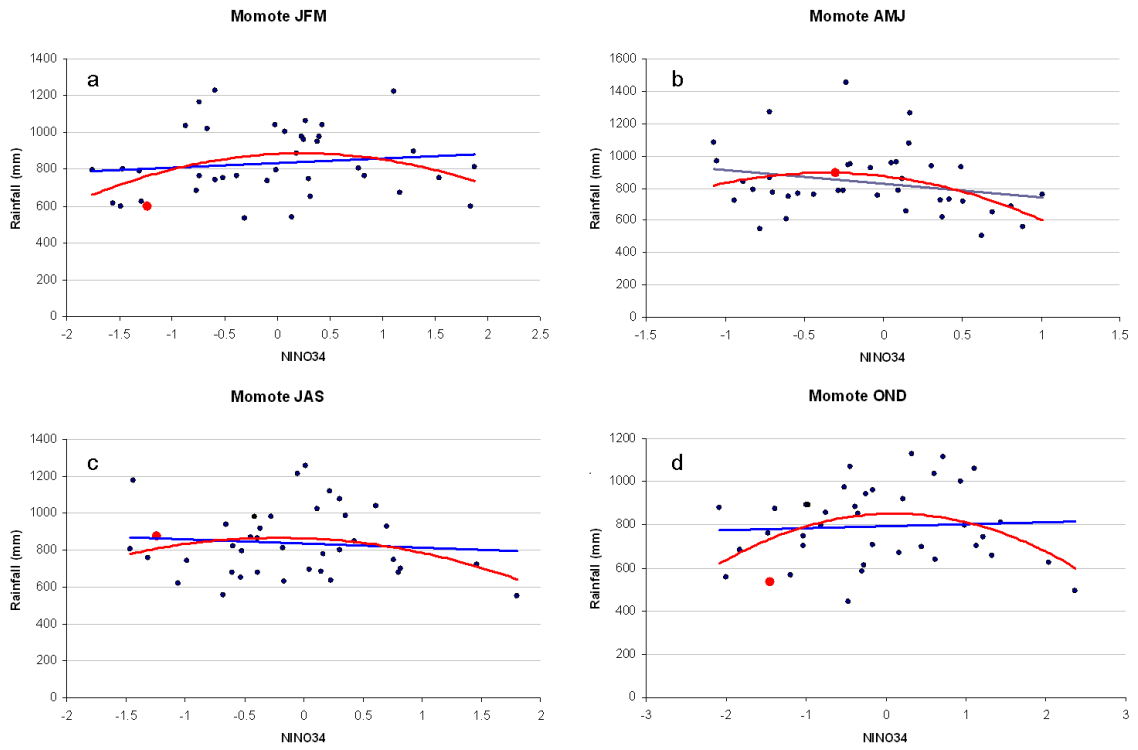

Figure 7.Scatter plots of Momote seasonal rainfall totals as a function of NINO34 SST anomalies: (a) JFM, (b) AMJ, (c) JAS and (d) OND. The blue lines represent linear fits to the data, the red curves represent second order polynomial fits to the data. The red symbol indicates the value associated with the 2010 to 2011 La Niña event (i.e. JAS 2010, OND 2010, JFM 2011 and MAM 2010).

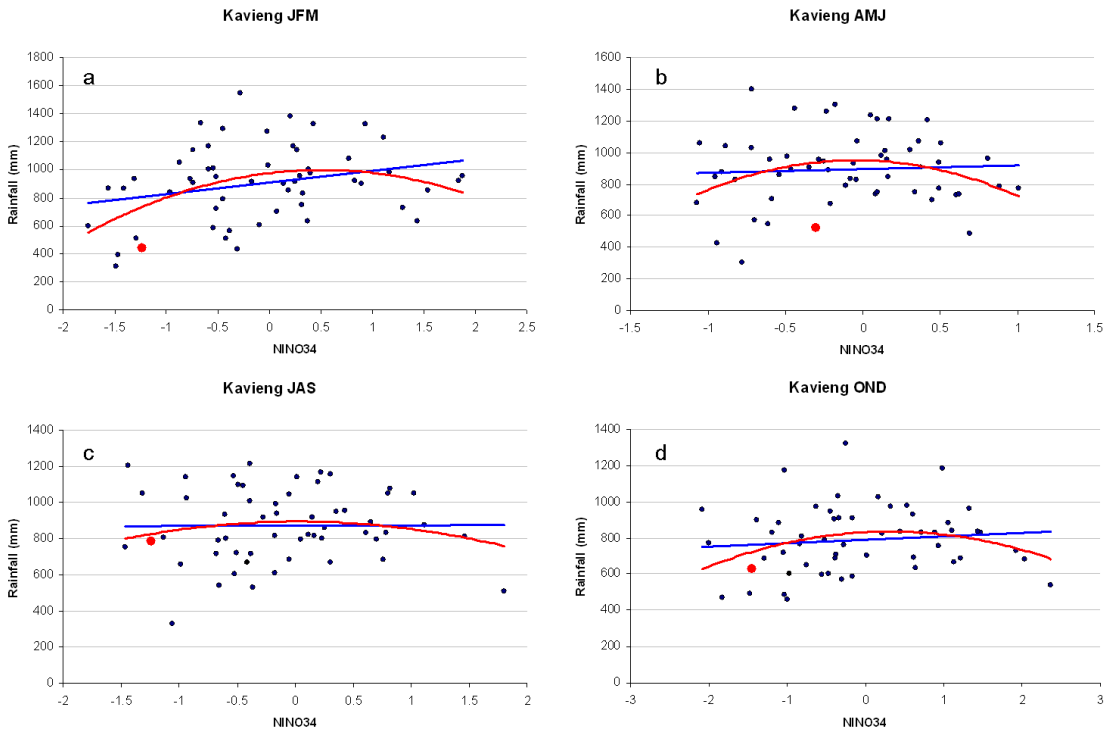

Figure 8.As for Figure 7 except for Kavieng.

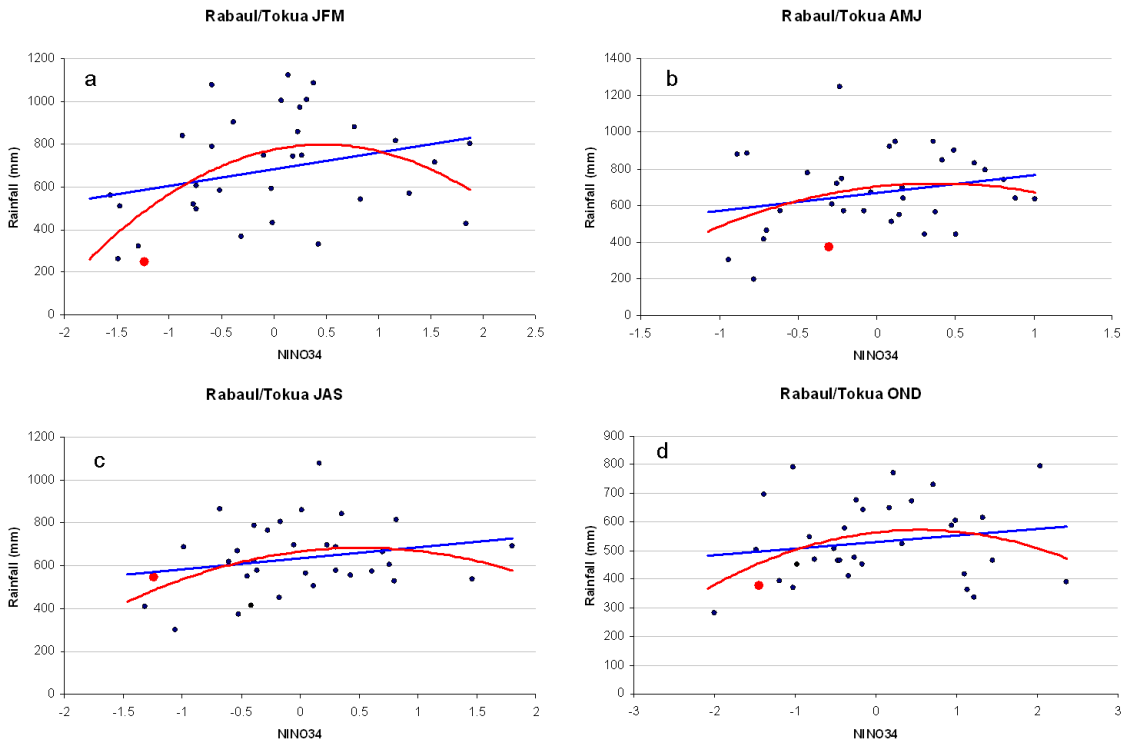

Figure 9.As for Figure 7 except for Rabaul/Tokua.

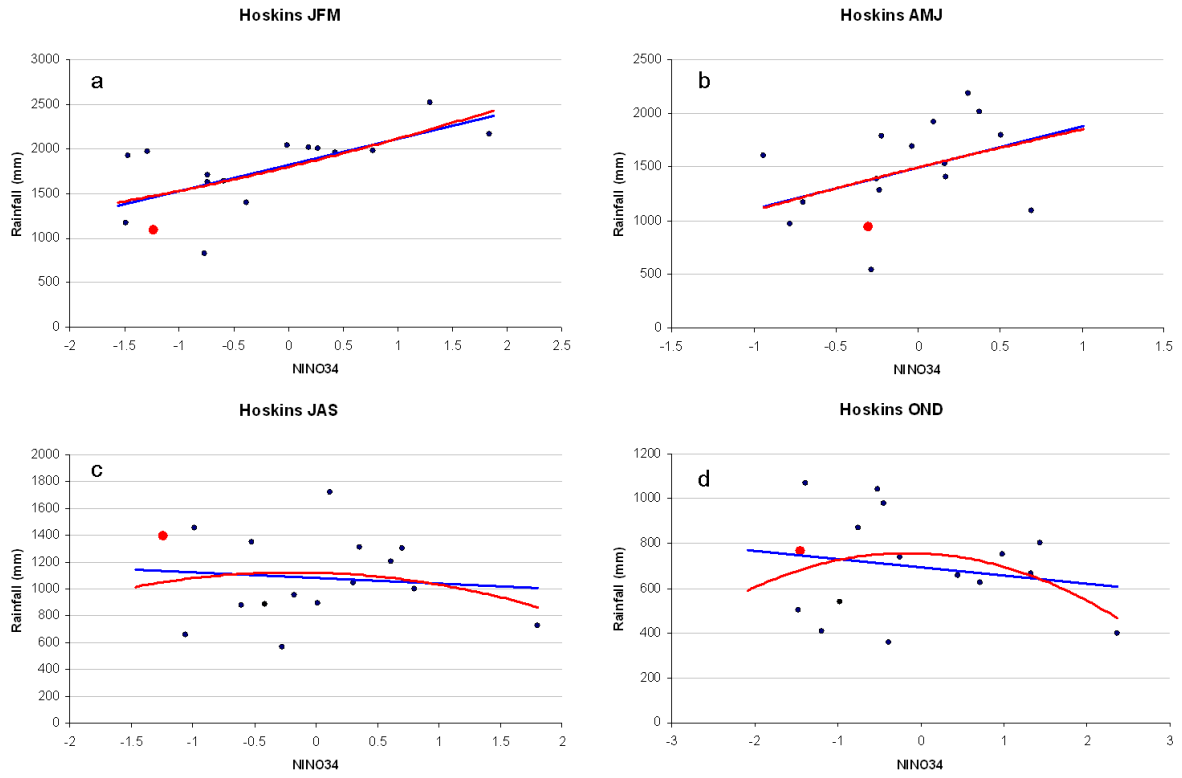

Figure 10.As for Figure 7 except for Hoskins.

Table 1

Product	**Major source**	**Resolution** (at the latitude of New Guinea)	**Period**	**Reference**
CMAP	Gauge and satellite	250 km	1980-2008	Xie, and Arkin (1997)
GPCPv2.2	Gauge and satellite	250 km	1980-2008	Adler et al. (2003)
NCEP1	Model	188 km	1949-present	Kalnay et al. (1996)
NCEP2	Model	188 km	1970-present	Kamitsu et al. (2002)
ERA40	Model	125 km	1980-2002	Bets and Baljaars (2003)
ERA-INT	Model	70 km	1980-2011	Dee et al. (2011)
MERRA	Model	50 km x 150 km	1980-2010	Bosilovich et al. (2008)
CFSR	Model	50 km	1980-2011	Saha et al. (2010)
GPCC (land only)	Gauges only	50 km	1901-2010	Schneider et al. (2011)
TRMM	Satellite	25 km	1999-2011	Huffman et al. (2007)

Table 2. The correlation between seasonal average NINO34 and seasonal rainfall. Values estimated to be significant at $p<0.05$ are bolded, those at $p<.01$ are also underlined. The second entry (where shown) refers to a second order polynomial fit to the data (note this is always positive) and the significance estimate takes into account the reduced degree of freedom in each sample.

Station (sample size, years)	JFM	AMJ	JAS	OND
Papua New Guinea sites				
Aiyura (60)	0.02	**0.63**	0.24	**0.40**
Daru (59)	0.01	-0.07	-0.20	**-0.35**
Goroka (46)	0.26	-0.09	-0.30	-0.24
Misima (62)	**-0.51**	**-0.26**	0.00	-0.14
Gurney (19)	**0.57**	**0.50**	-0.02	-0.09
Lae_Nadzab (23)	0.27	0.34	0.10	-0.06
Madang (61)	**0.29**	0.06	0.11	-0.11
Misima (62)	**-0.51**	**-0.26**	0.00	-0.14
Port Moresby (62)	-0.15	-0.14	-0.10	-0.08
Rumginae (36)	-0.29	-0.24	-0.31	**-0.67**
Vanimo (15)	0.29	0.38	-0.25	**-0.50**
Weewak (56)	-0.20	-0.14	-0.10	-0.08
New Ireland and New Britain sites				
Momote (55)	0.14 **0.34**	-0.20 **0.35**	-.04 0.25	0.08 **0.38**
Kavieng (55)	**0.27** **0.41**	0.06 **0.28**	0.01 0.15	0.11 **0.27**
Rabaul/Tokua (33)	0.29 **0.52**	0.24 0.30	0.22 **0.35**	0.17 0.32
Hoskins (16)	**0.66** **0.66**	0.40 0.40	-0.11 0.20	-0.19 0.32
West Irian sites				
Sentani (39)	0.06	0.20	-0.18	-0.07
Wamena (40)	0.07	-0.17	**-0.48**	**-0.47**
Agats (19)	-0.12	**-0.47**	-0.29	-0.40
Merauke (39)	0.21	-0.20	**-0.39**	-0.29